Comparative analysis of *Salmonella enterica* serovar Typhi isolates from acute and chronic infections

Undergraduate Thesis

Presented in partial fulfillment of the requirements for graduation with research distinction in Biomedical Science in the College of Medicine at The Ohio State University.

Bradley Eichar

Bachelor of Science in Biomedical Science

The Ohio State University

2018

Thesis committee:

John Gunn, Ph.D.; Advisor

Brian Ahmer, Ph.D.

Melissa Quinn, Ph.D.

Table of Contents

Acknowledgements

I would like to sincerely thank Dr. John Gunn for his mentorship, guidance, and support. It has been a privilege to work with him throughout my undergraduate career, and I am grateful for all the time and energy he has invested in me over the past four years. I would like to thank Juan Gonzalez and Mark Hahn for their assistance on this project. Additionally, I would like to thank past and present laboratory members including Dominique Olds, Erin Vasicek, Haley Adcox, Ky Hoang, Regan Hitt, Jenna Sandala, Jasmine Moshiri, Darpan Kaur, Victoria Koscuta, Laura Kuo, Lauren Tucker, and Natalie Cervelli for their support. I would also like to thank Steven Mousetes for his support, advice, and encouragement throughout the years. Thank you to our collaborators Dr. Stephen Baker, Dr. Steven Goodman, and Dr. Wondwossen Gebreyes. I would also like to thank my committee members Dr. Brian Ahmer and Dr. Melissa Quinn for taking time out of their busy schedules to allow me to present my thesis project.

Lastly, I would like to acknowledge the funding sources for this work, which include the National Institutes of Health, the SOLAR Research Fund, the Undergraduate Research Office, and the Biomedical Science program.

Chapter 1

Introduction

1.1 Problem Statement

Salmonella enterica (*S. enterica)* is a facultative, intracellular, gram-negative bacterium that causes serovar-specific disease in a range of hosts. In the human host, *S. enterica* serovars may cause typhoidal as well as non-typhoidal illness, both with significant global distribution. Non-typhoidal *S. enterica* causes gastroenteritis and is responsible for over 78 million cases globally of foodborne illness each year [1]. *Salmonella enterica* serovar Typhi (*S.* Typhi) is a human-specific pathogen and the primary etiologic agent of typhoid fever. *S.* Typhi infections are responsible for an estimated 21 million new infections each year, resulting in 200,000 deaths. Typhoid fever is an acute illness, frequently characterized by high fever, malaise, and abdominal pain. *S.* Typhi is of high clinical relevance in the regions of South-central Asia, South-eastern Asia, and Southern Africa [1].

Infection by *S.* Typhi is most commonly caused by the consumption of contaminated food or water. Once ingested, *S.* Typhi crosses the intestinal epithelial barrier where it is phagocytosed by macrophages, but replicates within these cells to achieve systemic infection. Common sites of the bacterium within the host include bone marrow, spleen, liver, and pancreas. From the liver, the bacterium is also able to transit to the gallbladder, the storage site for bile, through the vasculature or the ducts that emanate from the liver [2].

With appropriate treatment, most patients recover from the acute stage of the disease; however, 3-5% of individuals infected with *S.* Typhi develop a chronic infection in the gallbladder. An epidemiological study found that an important factor in the development of chronic gallbladder carriage is the presence of cholesterol gallstones – which can be found in 80-90% of carriers [3]. We have demonstrated that *S.* Typhi mediates carriage through the formation of biofilms on the surface of cholesterol gallstones in the gallbladder (Figure 1) [2].

Biofilms are organized multicellular communities encapsulated in an extracellular polymeric substance (EPS), comprised of secreted and cell wall-associated polysaccharides, proteins, and extracellular DNA. Bacteria within a biofilm are protected from external (e.g. antibiotics) and internal (e.g. innate immune response) factors [4, 5]. Biofilm development is characterized by sequential events which include surface attachment, secretion of the EPS, and dispersal of community members to the environment [6]. Biofilms in the intestine or gallbladder may also play a role in persistence of non-typhoidal gastroenteritis-causing *Salmonella* serovars.

The spread of *S.* Typhi can be linked to the carrier state during which fecal shedding allows the bacteria to be acquired by hosts through contaminated food/water. Individuals that become chronic *S.* Typhi carriers are asymptomatic and are direct threats to public health as they can unknowingly shed the bacteria in their feces and urine. Therefore, these patients often serve as critical reservoirs for maintaining the pathogen in a population. Additionally, the typhoid carrier state, both with and without the occurrence

of gallstones, is a crucial predisposing factor for the development of gallbladder cancer [7]. Because biofilm formation on cholesterol gallstones is a hallmark of chronic carriage, treating this state is extremely difficult and ineffective. Traditional therapy for carriage includes an antibiotic regimen with a cholecystectomy; however, while surgical gallbladder removal can be considered, in developing nations where typhoid is most prevalent, this invasive therapy is unavailable as a means for bacterial eradication.

The impact that chronic carriage has on human health, combined with the high global incidence of typhoid fever, highlights the significance of this research. This project is part of an ongoing effort to characterize the chronic carrier state of *S.* Typhi – with the goal of determining the mechanisms of chronic, asymptomatic *S.* Typhi carriage. This project examined clinical isolates from confirmed acute and chronic *S.* Typhi infections in a variety of biological, genetic, and molecular assays. The findings of this research will pave the way for targeted drug therapies that have the potential to reduce or eliminate the chronic carrier state of *S.* Typhi, thus alleviating the burden of typhoid fever.

1.2 Hypothesis and Rationale

We hypothesize that phenotypic and genomic differences exist between acute and chronic clinical isolates of *S.* Typhi. If the functional, molecular, or genetic characteristics of the strains differ, it may suggest that strain variations are linked to the ability to establish carriage. This hypothesis was examined through the following aims:

1. Examination of biofilm formation of acute and chronic strains.
2. Comparison of the exopolysaccharide matrix components of acute and chronic strains.
3. Analysis of the molecular and genetic typing of acute and chronic *S.* Typhi strains.

Chapter 2

Materials and Methods

2.1 Bacterial Strains and Growth Conditions

The bacterial strains used in this study were wild-type (WT) *S.* Typhi Ty2 (JSG698), *S.* Typhimurium ATCC 14028 (JSG210), and *S.* Typhi clinical isolates from patients with either an acute or chronic typhoidal infection (Table 1). All clinical *S.* Typhi isolates tested positive by Vi-antigen agglutination test before use in this study. The strains were streaked on Luria-Bertani (LB) agar plates and incubated at 37 ˚C overnight. Single colonies were used to start overnight (O/N) liquid cultures. Planktonic cells were grown at 37 ˚C on a rotating drum in LB or tryptic soy broth (TSB). Antibiotics, when needed, were used at the following concentrations: chloramphenicol, 25 μg/ml; ampicillin, 100 or 200 μg/ml, kanamycin, 45 μg/ml; and streptomycin, 100 μg/ml. The deletion of Δ*tviB* was generated by the λ-Red mutagenesis method [8] with the following primers: upstream primer JG2934 (ataaaattttagtaaaggattaataagagtgttcggtatagtgtaggctggagctgcttc), downstream primer JG2935 (gtccgtagttcttcgtaagccgtcatgattacaatctcaccatatgaatatcctccttag), upstream verification primer JG2936 (tcagcgacttctgttctattcaagtaagaaaaggggtacgg), and downstream verification primer JG2937 (gctcctcactgacggacgtgcgaacgtcgtctagattatg). Antibiotic resistance markers were swapped out using pCP20 [9]. The mutant was verified via PCR and electrophoretic gel analysis.

2.2 Molecular and Genetic Typing of Acute and Chronic *S.* Typhi Strains

S. Typhi strains from Ohio and Mexico City were assayed for relatedness using Pulsed-field gel electrophoresis (PFGE). Fresh, isolated single colonies were added to 2 ml of cell suspension buffer (CSB). The cells were re-suspended in 300 µl of Gram-negative lysis buffer and dispensed into the plug molds. Plugs were digested using SmaI. The standard markers, *Salmonella enterica* BAA-664 plugs, were also digested using XbaI at the same time. PFGE parameters used were a gradient of 6, run time of 18 h (h=hours), included angle of 120, initial switch time of 5 s (s=seconds), and final switch time of 40 s. After the run was complete, the gel was stained using 5 µl/ml of ethidium bromide in distilled water and photographed using Gel Doc 2000 (Bio-Rad). Images were analyzed using Bionumerics 4.0 (applied Math) using a Dice similarity coefficient and an unweighted-pair group method using average linkages (UPGMA) dendrogram type. Position tolerance settings included optimization at 1.50% and position tolerance at 2.0%.

Clinical *S.* Typhi strains acquired from Vietnam had been previously whole-genome sequenced before use in this study. All remaining isolates were whole-genome sequenced as part of a consortium with the U.S. Food and Drug Administration (FDA), who agreed to sequence 1,000 clinical isolates from the U.S., Mexico, Thailand, east Africa, and Brazil. The maximum-likelihood phylogenetic tree was built from the SNP alignment of all 22 isolates, *S.* Typhi Ty 2 (JSG698), and Typhimurium 14028s (JSG210) strain included as an outgroup for tree rooting, using RAxML (version 7.8.6)55 with the generalized time-reversible model and a Gamma distribution to model site-specific rate variation (the GTR+Γ substitution model; GTRGAMMA in RAxML). Support for the

maximum-likelihood phylogeny was assessed via 100 bootstrap pseudoanalyses of the alignment data.

2.3 Biofilm Growth and Crystal Violet Assays

S. Typhi cultures were grown overnight (O/N) in TSB at 37 ˚C with aeration. Cultures were then normalized to OD_{490} = 0.65, diluted 1:6 in TSB, and incubated for 3 hours at 37 ˚C, static. Bacteria were then diluted 1:2500 and 200 µl of the bacterial suspension were dispersed into non-treated polystyrene 96-well plates (Corning, Kennebunkport, ME). The plates were incubated at 30 ˚C in a GyroMini nutating mixer (LabNet International, Inc., NJ) at 24 rpm for 96 h. To simulate growth conditions on gallstones, wells were pre-coated with cholesterol by adding a solution of 5 mg/mL in 1:1 isopropanol:ethanol and air-dried overnight. Media was changed daily for biofilm growth. After 96 hours, plates were washed 4 times in ddH_2O to eliminate planktonic cells. Biofilms were heat fixed 1 hour at 60 ˚C, stained with .33% crystal violet solution (6.0 ml PBS, 3.3 ml crystal violet, 333 µl methanol, 333 µl isopropanol) for 5 minutes, and released using 33% acetic acid (3.3 ml glacial acetic acid, 6.7 ml ddH_2O) to quantify the stain. Biofilm quantification was performed by measuring the optical density (OD_{570}) of the released dye in a SpectraMax spectrophotometer with SoftMax Pro software (Molecular Devices, Sunnyvale, CA) to determine the amount of dye retained, which correlates to the amount of biofilm present.

2.4 Dot Blot Assay

Bacterial cultures were grown overnight in TSB at 37 ˚C with aeration, fixed in 4% paraformaldehyde (PFA), and normalized to OD_{600} = 0.8 in PBS. Normalized cultures were then divided into a lysate group and a non-lysate group. Lysate cultures were boiled for 10 min to break apart the cells. Bacterial dilutions (1:6 for Vi antigen; 1:20 and 1:50 for LPS) were prepared, spotting 200 µl onto methanol-activated PVDF membranes using a suction manifold device. The blots were dried and blocked at 4 ˚C O/N with 5% milk buffer, followed by incubation in either α-Vi-antigen (1:1000) or α–LPS (1:1000). The blots were washed 3 times, 15 minutes each, in tris-buffered saline with polysorbate 20 (TBST) and incubated with anti-mouse (for LPS; 1:2:000) or anti-rabbit (for Vi; 1:2000) horseradish peroxidase-conjugated secondary antibodies (Bio-Rad) O/N at 4 ˚C prior to visualization using the Bio-Rad Chemi-Doc XRS system.

2.5 Congo Red Assay

Congo Red agar plates were prepared using LB-no salt supplemented with Congo Red (40 µg/ml) and Coomassie Brilliant Blue (20 µg/ml). Bacterial suspensions were created from single colony streaks on LB agar plates, diluted 1:100 in LB-no salt, and normalized to OD_{600} = 5. Cultures were plated by dropping 5 µl onto the Congo Red plates and incubating for 24 to 48 hours at 30 ˚C.

2.6 Confocal Microscopy of Biofilms

S. Typhi strains were inoculated from a frozen stock into TSB broth and grown overnight at 37°C with aeration. Cultures were then normalized to OD_{490} = 0.65, diluted 1:6 in TSB, and incubated for 3 hours at 37 ˚C, static. Bacteria were then diluted 1:2,500 and 200 µl of the bacterial suspension was added to each well of a LabTek II 8-well chambered coverglass (LabTek). Slides were incubated static for 16 hrs at 37°C in a humidified atmosphere at which time medium was aspirated and replaced with fresh TSB broth. After an additional 8 hrs (24 hrs total incubation time), medium was aspirated and replaced with fresh TSB broth. After an additional 16 hours (40 hours total incubation time), biofilms were then stained with LIVE/DEAD® *Bac*Light™ Bacterial Viability kit for microscopy (Molecular Probes), then fixed with a solution of 16% paraformaldehyde-2.5% glutaraldehyde- 4% acetic acid in 0.2M phosphate buffer, pH 7.4, prior to immediate imaging by confocal microscopy. Z-stack images were collected via confocal microscopy and analyzed by COMSTAT2 to quantify average thickness and mean biomass.

Chapter 3

Results

3.1 Molecular and Genetic Typing of Acute and Chronic *S.* Typhi Strains

S. Typhi isolates from Ohio and Mexico City were assayed for relatedness using Pulsed-field gel electrophoresis (PFGE). Subtyping by PFGE with the restriction enzymes XbaI and SmaI showed that isolates from Ohio had different banding patterns shown in Figure 1. Of the 11 isolates subtyped, there were a total of seven different PFGE patterns. Four acute carrier isolates from Ohio (JSG3400, JSG3418, JSG3419, and JSG3431) had unique banding patterns not shared by other isolates. Chronic carrier isolates from Mexico, JSG3074 and JSG3076, demonstrated identical PGFE patterns. Additionally, two pairs of Ohio acute isolates (JSG3433 and JSG3441; JSG3395 and JSG3407) also demonstrated identical PGFE patterns. Overall, the majority of isolates (90%) demonstrated high similarity according to PGFE phylogenetic analysis (≥85.7% similar). Ohio acute isolate JSG3400 was the most unique isolate from the group (≥64.2% similar).

In order to make better phylogenetic comparisons, we whole-genome sequenced all of the Ohio and Mexico City *S.* Typhi isolates under study, as well as newly acquired Vietnam isolates. The resulting maximum-likelihood phylogenetic tree is shown in Figure 2. Clinical isolates displayed high genetic similarity with multiple tight clusters formed. Genome-sequencing analysis, as observed in the PFGE, also revealed acute JSG3400 as an outlier from the group. However, there were no clusters formed based on geographical location of the isolates or the carrier status of the patients.

3.2 Crystal Violet Biofilm Studies

In order to assess the general biofilm forming abilities of chronic carrier and acute isolates, we performed a biofilm assay on cholesterol-coated polypropylene plates for 96 h. Cholesterol-coated plates mimic the cholesterol surface found on gallstones where biofilms are formed in chronic carriers. The strains examined included the eight chronic carrier isolates, 14 isolates from acute patients, WT *S.* Typhi, and a Vi-antigen mutant – JSG4123 (Δ*tviB)*. The crystal violet biofilm assay revealed variable biofilm formation across all isolates as illustrated in Figure 3. No patterns emerged regarding the site at which the strains were cultured in acutely or chronically infected patients.

3.3 Dot Blot Assay

Comparison of the extracellular matrix components, Vi-antigen and lipopolysaccharide (LPS), of acute and chronic strains were completed by dot blot analysis. Dot blot studies of Vi-antigen revealed variable expression across all isolates shown in Figure 4A. Negative controls included JSG210 (*S.* Typhimurium) and Vi-antigen mutants JSG4123 and JSG1213. There was no clear pattern of expression between acute or chronic isolates. Acute isolates JSG3989, JSG3395, and JSG3418 demonstrated high Vi-antigen expression on the whole cell, while chronic isolates JSG3983 and JSG3982 also revealed high whole cell Vi expression. Additionally, WT *S.* Typhi demonstrated high whole cell detection of Vi-antigen. All remaining clinical isolates, both acute and chronic, demonstrated weak to no Vi-antigen detection. This result was additionally confirmed by Vi agglutination tests (data not shown). In many isolates, Vi-antigen was not detected on the surface or in the lysate preparations.

LPS detection by dot blots (Figure 4B) also revealed variable expression on both the surface and in the lysate preparations. Like the Vi-antigen assay, there was no clear pattern of expression when comparing acute and chronic isolates. Acute isolate strains JSG3989, JSG3987, and JSG3400 demonstrated high LPS expression both on the surface and in the lysate preparations. However, there was no LPS detected in either preparations in chronic carrier isolate strains JSG3074, the Vi-mutant JSG4123, JSG3982, and acute isolate strain JSG3407. LPS was only detected in the lysate of the remaining isolates. WT *S.* Typhi had low whole cell detection of LPS with high detection in the lysate preparation. However, high levels of LPS were detected on the surface of the WT *S.* Typhi Vi mutant, JSG1213.

3.4 Confocal Microscopy Examination of Biofilms

To examine if there were differences in biofilm architecture between chronic and acute isolates, we utilized confocal microscopy to measure thickness (μm) and biomass ($\mu m^3/\mu m^2$). Z-stack images were captured of chronic and acute isolate biofilms grown for 40h and analyzed with COMSTAT2© software. In measurements of average thickness, chronic carrier isolates formed thicker biofilms than acute isolates as shown in Figure 5. Likewise chronic isolates, formed more biomass than acute carrier isolates (Figure 6).

3.5 Cellulose and Curli Fimbriae Detection

To detect cellulose and curli fimbriae in the isolates, a Congo red (CR) binding assay was utilized (Figure 7). CR is a hallmark amyloid-binding dye that binds to curli, as well as to cellulose. JSG210 (*S.* Typhimurium) is known to produce high levels of curli and cellulose; therefore, it was used as a positive control. Clinical isolates plated on CR agar did not demonstrate the red, dry, and rough (rdar) phenotype compared to *S.* Typhimurium. However, *S.* Typhi WT and clinical isolates were pink, dry, and rough (pdar), suggesting that they produce cellulose but not as much curli as *S.* Typhimurium. There were variable morphotypes between the colonies, but no clear pattern emerged based on location source of isolates or carrier status of infected patients.

Chapter 4

Discussion

The spread of *S.* Typhi is dependent on the chronic carrier state during which fecal shedding allows bacteria to spread to new hosts through contamination of water sources. The *S.* Typhi chronic carriage state includes the formation of biofilm communities on the surface of gallstones in the gallbladder. Further understanding of the biological mechanisms involved in carriage is critical to impeding the burden of typhoid fever.

Differences in *S.* Typhi isolates may account for clinical outcomes in patients. In this present study, we hypothesized that phenotypic and genomic differences exist between acute and chronic clinical isolates of *S.* Typhi. This hypothesis was tested by (1) examination of biofilm formation of acute and chronic strains, (2) comparison of the exopolysaccharide matrix components of acute and chronic strains, (3) analysis of the molecular and genetic typing of acute and chronic *S.* Typhi strains.

4.1 Molecular and genetic typing of acute and chronic *S.* Typhi strains

In a preliminary study, we conducted Pulsed-Field Gel Electrophoresis (PFGE) of clinical isolates from the Ohio Department of Health and Mexico City. PFGE analysis revealed high genetic similarity between a majority of the isolates (85.7% similar), with one acute isolate, JSG3400, being a unique outlier from the group (64.2% similar to the group). To make more accurate phylogenetic comparisons, our isolates were whole-genome sequenced. Analysis of the sequences of all isolates revealed high similarity

between strains, confirming the results seen in the PFGE analysis. Similar to the PFGE result, JSG3400 was revealed as an outlier from the group in the whole-genome sequencing analysis. Phylogenetic comparisons of the sequences revealed that isolates were not clustered based on geography or carrier status.

The stability of the *S.* Typhi genome and relatedness of clinical strains, however, is a heavily debated topic. Previous studies have characterized the *S.* Typhi genome as highly clonal. Similarly, isolates from acute and chronic infections have been shown to exhibit minimal genetic variation or recombination [10, 11]. Despite this, some studies have reported conflicting data, such as the presence of variant *S.* Typhi strains with novel pathogenic elements and chromosomal rearrangements[12, 13]. Furthermore, chronic carriers have even been shown to simultaneously excrete *S.* Typhi strains with considerable genetic variation[14]. While genomic variants of *S.* Typhi may exist, our data suggests that clinical isolates, regardless of geography or infection status, are closely related and clonal in nature. However, as shown in the PFGE and maximum-relatedness tree, acute isolate JSG3400 did demonstrate genomic variability with aligns with the perspective that *S.* Typhi is not as clonal as we once believed.

4.2 Examination of Biofilm Formation

To characterize general biofilm forming abilities of the acute and chronic isolates, we utilized a crystal violet biofilm assay on cholesterol-coated 96-well polystyrene plates to quantify biofilm formation. Results from this experiment revealed variable biofilm

formation from both acute and chronic carrier isolates, with neither group forming superior biofilms than the other.

We further examined the biofilm forming abilities of the isolates, utilizing confocal microscopy. Z-stack images captured the biofilm architecture, measuring both thickness (μm) and biomass ($\mu m^3/\mu m^2$). Despite what crystal violet biofilm studies showed, chronic carrier isolates, on average, formed higher levels of biofilm by the measurements previously described. These data indicate that carrier isolates are able to form superior biofilms despite high genetic similarity to acute isolates. The crystal violet assay has a lot of utility as an easy and rapid biofilm measuring technique, which merits its use primarily in the high-throughput screening of anti-biofilm compounds. However, because the technique measures the retention of dye, it does not allow for the precise measurement of biofilm architecture. While our crystal violet data suggests that there is no difference in the biofilm forming abilities of *S.* Typhi clinical isolates, we are inclined to trust the more sensitive approach of confocal microscopy which demonstrated a remarkable difference in both the thickness and biomass of the biofilms.

4.3 Extracellular Matrix Studies

In this study, we used dot blots to compare the extracellular matrix components Vi-antigen and lipopolysaccharide (LPS) of acute and chronic strains. The production of Vi-antigen by *S.* Typhi is a distinguishing feature of the bacterium and the detection of Vi by agglutination is a common diagnostic procedure. Vi-antigen has been shown to have anti-phagocytic and anti-opsonic effects in the host [15]. Specifically, expression of Vi has

been shown to prevent complement receptor 3 (CR-3) dependent clearance and reduce bacterial-guided neutrophil chemotaxis through multiple pathways [16,17,18]. LPS is a major component of the outer membrane in gram-negative bacteria and plays a vital role in host-pathogen interactions with the innate immune system [19].

Dot blot assays of Vi-antigen expression revealed variable expression in both acute and chronic isolates. Three acute isolates (JSG3989, JSG3395, and JSG3418) and two chronic isolates (JSG3983 and JSG3982) demonstrated high Vi detection on the surface of the cell. WT *S.* Typhi (Ty 2) also demonstrated high Vi expression. The majority of the clinical isolates, both acute and chronic, expressed low Vi-antigen or were Vi-negative, despite testing positive for Vi by an agglutination test when the strains were originally received (data not shown). *S.* Typhi isolates lacking Vi-antigen have previously been reported, and it is thought that long-term storage of strains may lead to Vi-positive strains becoming Vi-negative [20]. However, strains that tested negative by the dot blot assay and agglutination test, were confirmed to be Vi-positive by PCR of the *tviB* gene. These data suggest that either Vi is missing due to mutations in the genes encoding Vi-antigen or that Vi is potentially modified and expression is regulated differently in various strains, despite how genetically similar whole-genome sequencing demonstrated these strains to be.

LPS dot blots were meant to be a control that should show uniformity across all isolates, but instead revealed unexpected variable expression on both the whole cell and in lysate preparations. Whole cell and lysate preparations were tested to determine if LPS

was present, but not being detectable on the surface due to modifications or steric hindrance by another surface molecule. While no clear pattern of LPS expression was seen in the acute or chronic group, only three acute isolates (JSG3989, JSG3987, and JSG3400) had detectable LPS on the surface of the cell. While WT *S*. Typhi had detectable levels of LPS on the surface, the Vi mutant of WT *S.* Typhi (JSG1213) had increased surface levels of LPS, suggesting that high Vi-antigen expression may be sterically blocking LPS detection. However, this same result was not seen in the chronic isolate JSG3074 and the chronic carrier Vi-mutant JSG4123 (Δ*tviB*). There was low Vi-antigen baseline expression for chronic isolate JSG3074 prior to Vi deletion, possibly suggesting that Vi antigen needs to be more abundant in order to block surface LPS detection. However, acute isolate JSG3939 showed both high levels of Vi and LPS suggesting that high Vi does not always correlate with low or no LPS detection.

Modifications made to the LPS molecule may be responsible for the lack of detection. LPS is known to be a key virulence factor in host–pathogen interactions and in the establishment of chronic infections. Previous studies have shown that alterations in the LPS molecule (e.g. modifications to the O antigen) contribute to host colonization, immune defense evasion, and adaptation to the infection niche[19,21,22].

Finally, we looked at cellulose and curli fimbriae production utilizing a Congo red assay. As filamentous appendages, curli fimbriae have highly adhesive properties and are an important component in the extracellular matrix. These fibers, along with cellulose expression, have been previously shown to be critical in initial adhesion of the bacterial

cells to surfaces, cell aggregation, pellicle formation, and biofilm formation [23,24, 25, 26, 27]. All 22 clinical isolates demonstrated a pink, dry, and rough (pdar) phenotype which is indicative of cellulose production but low curli production. *S.* Typhimurium however, demonstrated high levels of both curli and cellulose with a characteristic rough, dry, and red (rdar) phenotype. There was however, unexpected variability in the colony morphotypes as well.

4.4 Conclusions and Future Directions

In conclusion, these data suggest that despite the high genetic similarity seen between these clinical isolates, there is considerable phenotypic variability. While much of this variability could not be assigned to carrier status, chronic carrier isolates did demonstrate superior biofilm formation than the acute isolates. In future studies, we hope to elucidate the mechanism behind this result. Validation of the Vi-antigen and LPS dot blot data with immunofluorescence microscopy is also ongoing. After this, we would like to characterize the specific mutation or modifications made to both of these extracellular molecules. Overall, it is our hope that the findings outlined in this thesis will lead to a better understanding of the chronic carrier state of *S.* Typhi, and may one day yield effective and novel therapies to eliminate chronic *Salmonella* carriage.

Strain	Characteristics	Reference
JSG698	*S.* Typhi Ty2; wild-type	ATCC
JSG1213	*S.* Typhi Ty2 *tviB::Kan*	Gift of Popoff lab
JSG210	*S.* Typhimurium 14028s; wild-type	ATCC
JSG4123	JSG3074 Δ*tviB* via Wanner	This study
JSG3990	*S.* Typhi isolate; acute infection; Vietnam	Gift of S. Baker
JSG3989	*S.* Typhi isolate, acute infection; Vietnam	Gift of S. Baker
JSG3988	*S.* Typhi isolate, acute infection; Vietnam	Gift of S. Baker
JSG3987	*S.* Typhi isolate, acute infection; Vietnam	Gift of S. Baker
JSG3986	*S.* Typhi isolate, acute infection; Vietnam	Gift of S. Baker
JSG3985	*S.* Typhi isolate, acute infection; Vietnam	Gift of S. Baker
JSG3984	*S.* Typhi isolate, chronic carrier; Vietnam	Gift of S. Baker
JSG3983	*S.* Typhi isolate, chronic carrier; Vietnam	Gift of S. Baker
JSG3982	*S.* Typhi isolate, chronic carrier; Vietnam	Gift of S. Baker
JSG3981	*S.* Typhi isolate, chronic carrier; Vietnam	Gift of S. Baker
JSG3980	*S.* Typhi isolate, chronic carrier; Vietnam	Gift of S. Baker
JSG3979	*S.* Typhi isolate, chronic carrier; Vietnam	Gift of S. Baker
JSG3074	*S.* Typhi isolate, chronic carrier; Mexico City, Mexico	General Hospital of Mexico
JSG3076	*S.* Typhi isolate, chronic carrier; Mexico City, Mexico	General Hospital of Mexico
JSG3395	*S.* Typhi isolate, acute infection; Ohio (blood)	Ohio Department of Health
JSG3400	*S.* Typhi isolate, acute infection; Ohio (bile)	Ohio Department of Health
JSG3407	*S.* Typhi isolate, acute infection; Ohio (stool)	Ohio Department of Health
JSG3418	*S.* Typhi isolate, acute infection; Ohio (stool)	Ohio Department of Health
JSG3419	*S.* Typhi isolate, acute infection; Ohio (blood)	Ohio Department of Health
JSG3431	*S.* Typhi isolate, acute infection; Ohio (stool)	Ohio Department of Health
JSG3433	*S.* Typhi isolate, acute infection; Ohio (blood)	Ohio Department of Health
JSG3441	*S.* Typhi isolate, acute infection; Ohio (stool)	Ohio Department of Health

Table 1. Bacterial strains and relevant characteristics

Figures

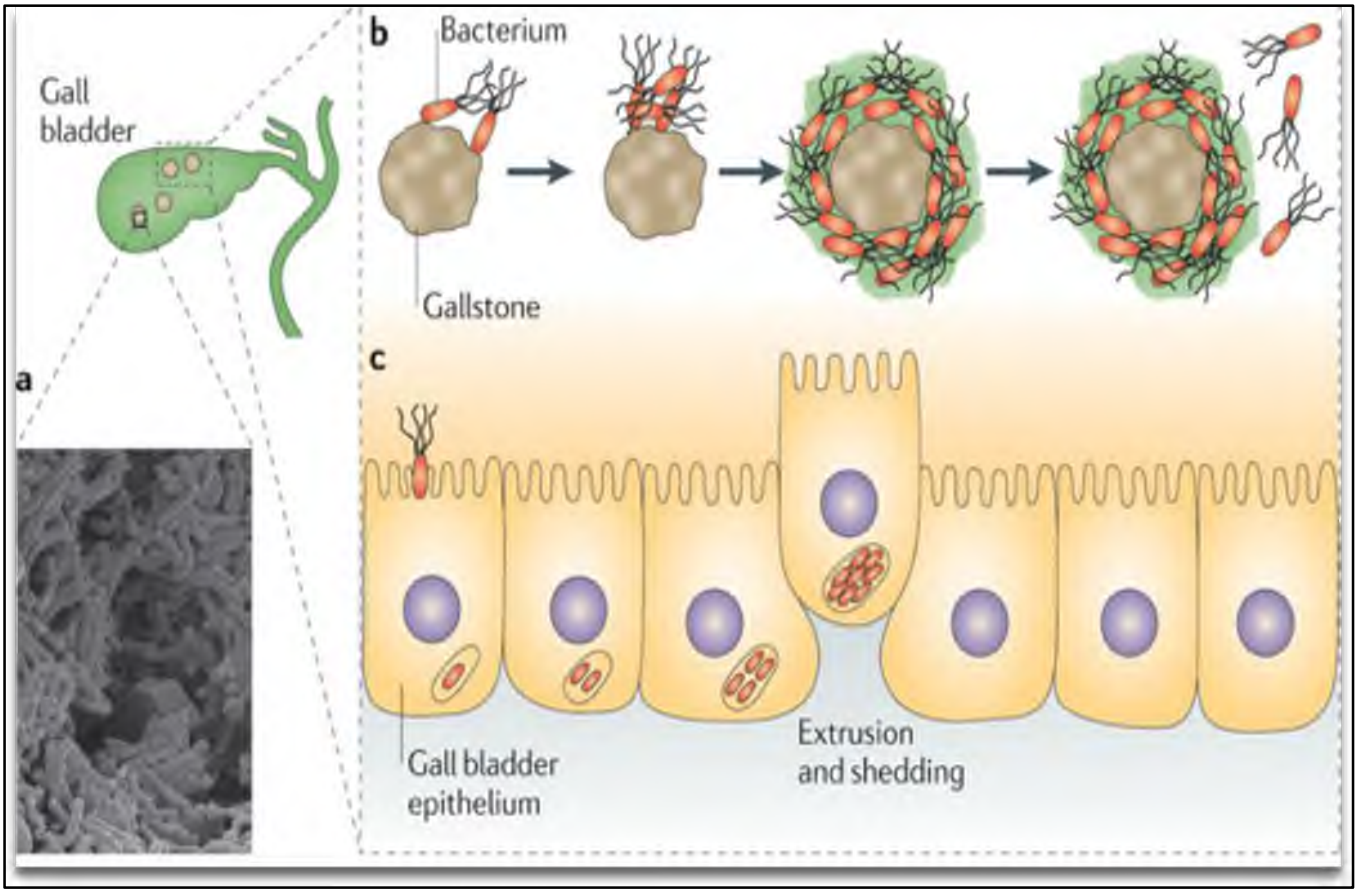

Figure 1. Model of *S.* Typhi chronic carriage. A) Electron micrograph of *S.* Typhi in a biofilm on the surface of a human gallstone. B) Schematic of *S.* Typhi biofilm formation on cholesterol gallstones in the gallbladder and shedding of bacteria. C) Schematic of *S.* Typhi infecting gallbladder epithelium, which leads to extrusion and shedding. Gonzalez-Escobedo G, Marshall JM, Gunn JS. Chronic and acute infection of the gall bladder by *Salmonella* Typhi: understanding the carrier state. *Nature Reviews Microbiology*. 2011;9(1):9-14. doi:10.1038/nrmicro2490.

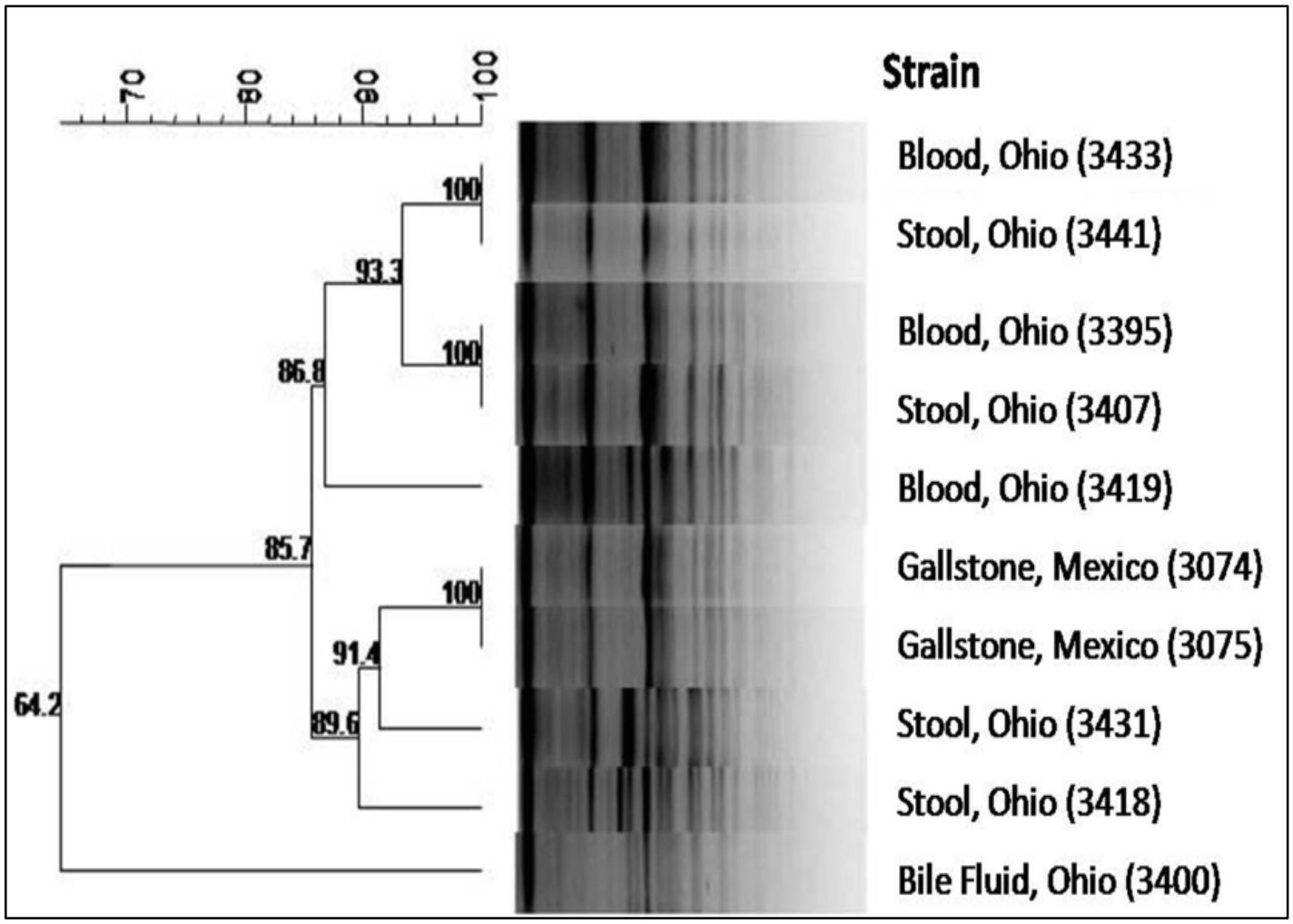

Figure 2. Results of Pulsed-Field Gel Electrophoresis (PFGE). Dendrogram showing genetic relationships among 10 *S.* Typhi clinical isolate strains based on PFGE patterns. The strains were compared using Dice index and clustered by the UPGMA method.

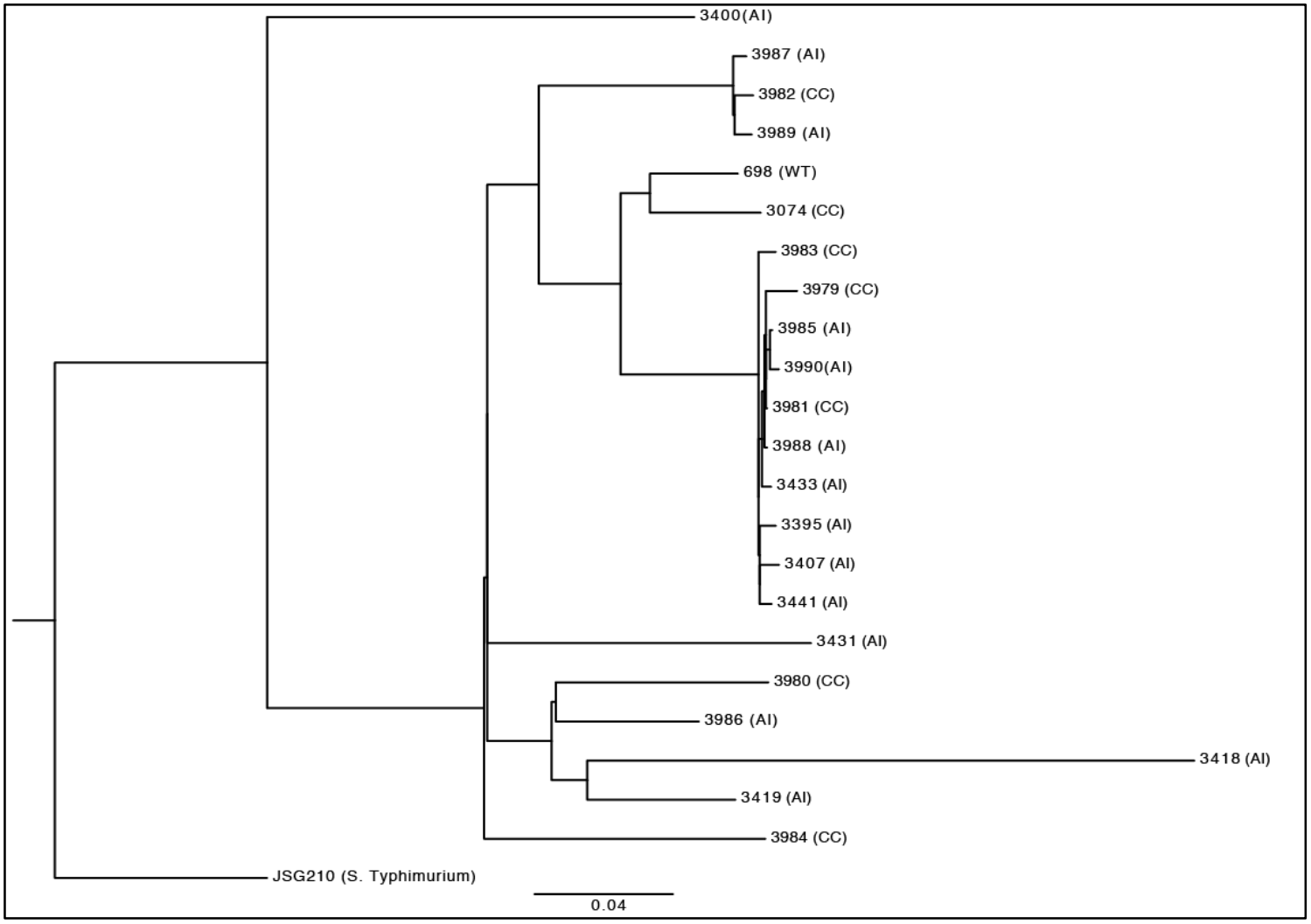

Figure 3. Maximum-likelihood phylogenetic tree. Dendrogram showing genetic relationships among all *S.* Typhi clinical isolate strains (CC: chronic carrier; AI: acute isolate) and JSG698 (WT) based on whole-genome sequences. JSG210 (*S.* Typhimurium) was used as outgroup for tree rooting.

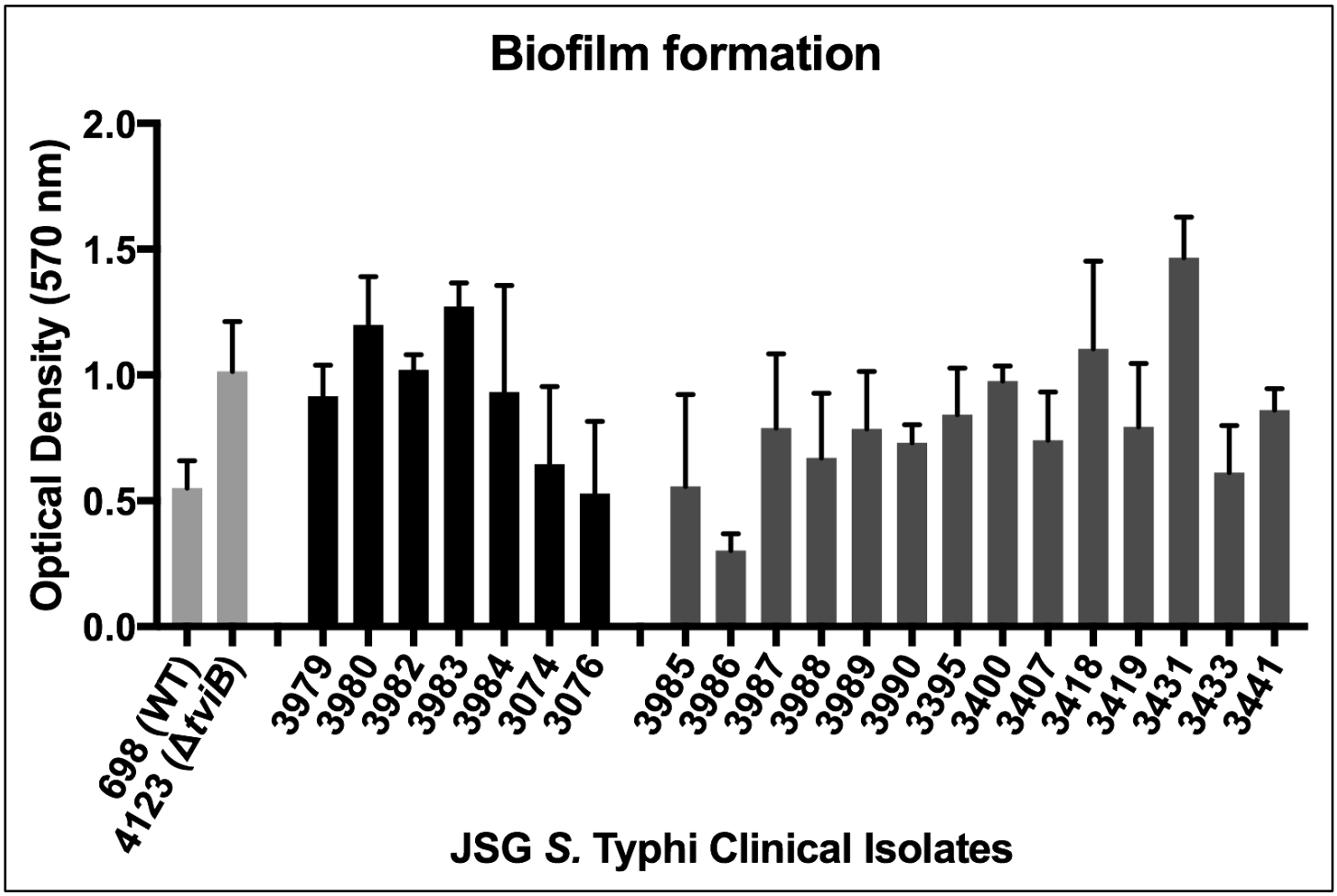

Figure 4. Analysis of biofilms with the crystal violet assay. Results of crystal violet biofilm assay with all 22 *S.* Typhi clinical isolates, JSG698 (WT), and JSG4123 (Δ*tviB*). Biofilms were visualized with crystal violet dye after 96h. Chronic carrier isolates are shown in black and acute isolates in charcoal. This biofilm assay was completed three times, with three technical replicates for each strain.

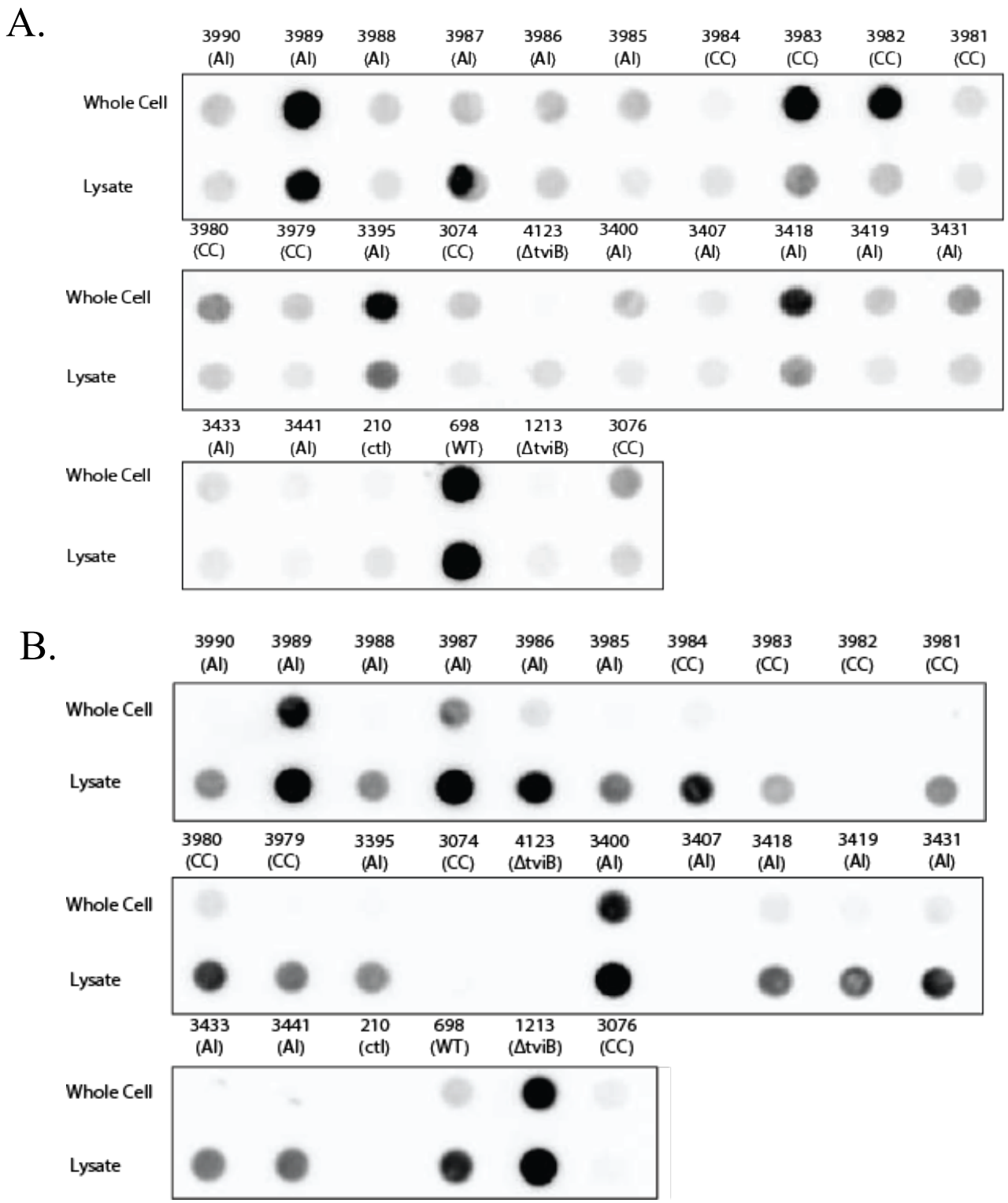

Figure 5. Results of dot blot assay. A) Image of Vi-antigen dot blot assay with all 22 clinical isolates (CC: chronic carrier; AI: acute isolate), JSG698 (WT), negative-control strain JSG210 (*S.* Typhimurium; ctl: control), and Vi-mutants JSG4123 and JSG1213. Whole cell and lysate preparations were diluted 1:6 in 1X PBS after normalization, division, and lysis step. B) Image of LPS dot blot assay. Preparations were diluted 1:20 in 1X PBS after normalization, division, and lysis step.

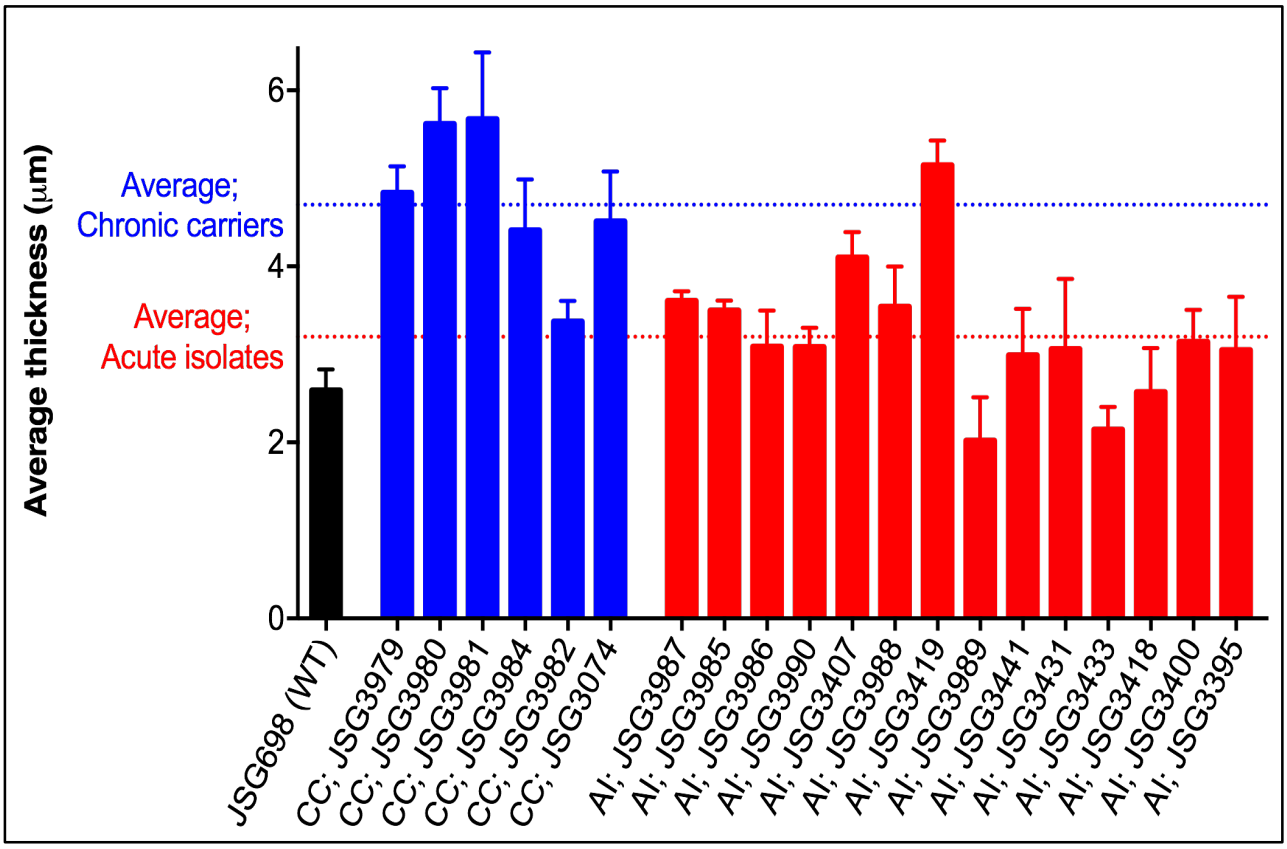

Figure 5. **Confocal analysis of biofilms.** Average thickness (μm) of all clinical isolates (CC: chronic carrier; AI: acute isolate) and JSG698 (WT). Chronic carrier isolates are shown in blue and acute isolates are shown in red. Z-stack images were captured of chronic and acute isolate biofilms grown for 40h and analyzed with COMSTAT2 software.

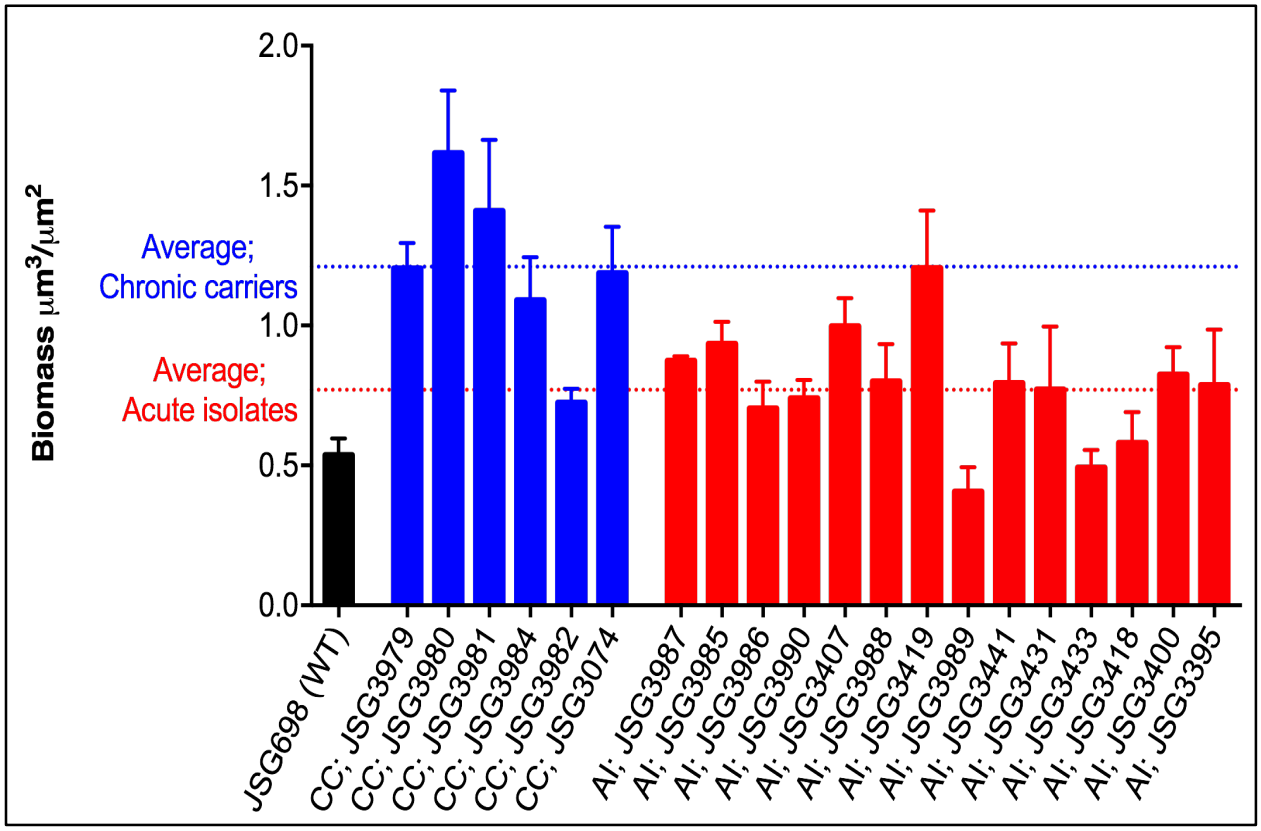

Figure 6. Confocal analysis of biofilms. Average biomass ($\mu m^3/\mu m^2$) of all clinical isolates (CC: chronic carrier; AI: acute isolate) and JSG698 (WT). Chronic carrier isolates are shown in blue and acute isolates are shown in red. Averages of each group, carrier and acute isolates, are seen marked by dashed-line. Z-stack images were captured of chronic and acute isolate biofilms grown for 40h and analyzed with COMSTAT2 software.

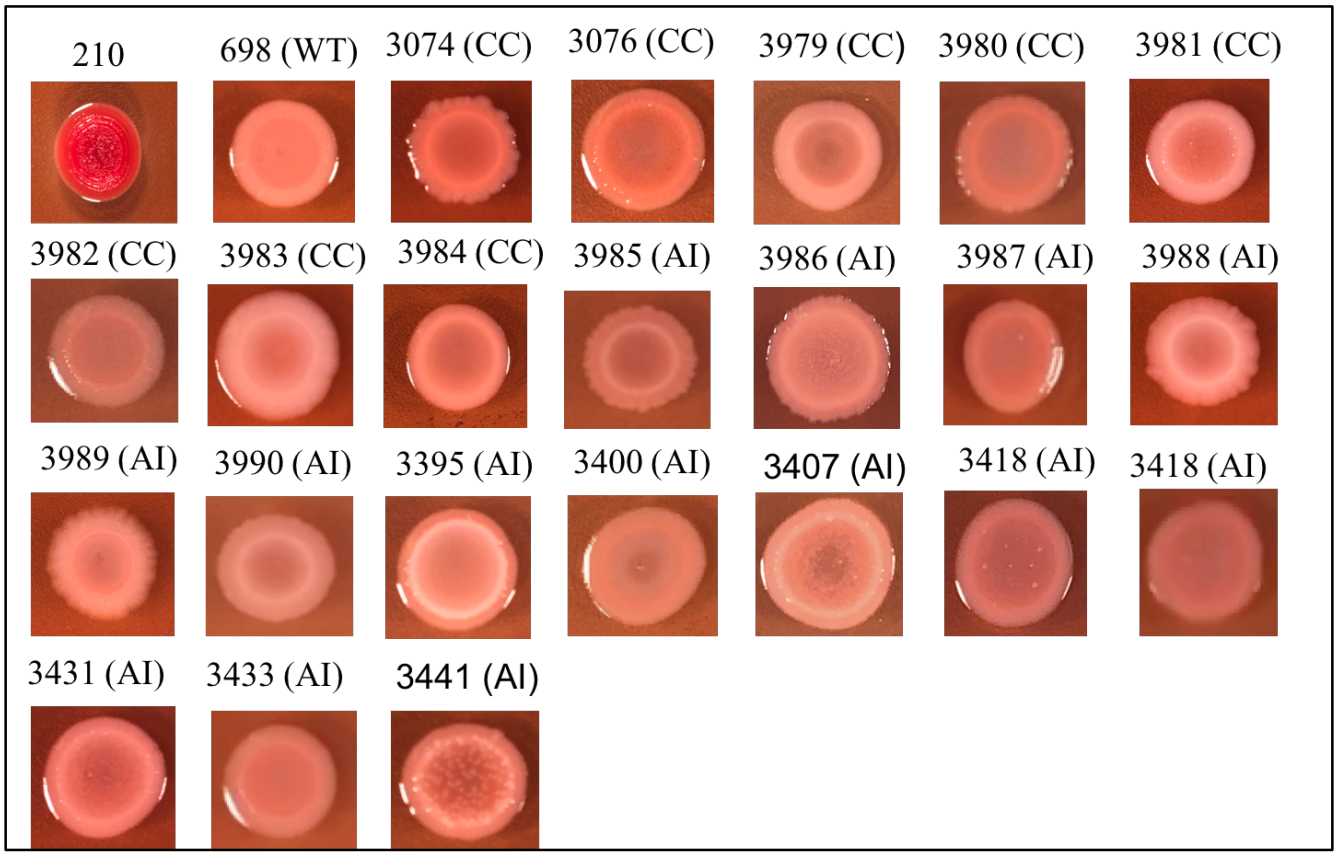

Figure 7. Congo Red Agar Assay. Images of all 22 clinical isolates (CC: chronic carrier; AI: acute isolate), positive control JSG210 (*S.* Typhimurium), and JSG698 (WT).

References

1) Crump JA, Mintz ED. Global trends in typhoid and paratyphoid fever. Clinical infectious diseases : an official publication of the Infectious Diseases Society of America. 2010;50(2):241-246. doi:10.1086/649541.

2) Adcox HE, Vasicek EM, Dwivedi V, Hoang KV, Turner J, Gunn JS. Salmonella extracellular matrix components influence biofilm formation and gallbladder colonization. Infect Immun. 2016.

3) Gonzalez-Escobedo G, Marshall JM, Gunn JS. Chronic and acute infection of the gall bladder by Salmonella Typhi: understanding the carrier state. Nature Reviews Microbiology. 2011;9(1):9-14. doi:10.1038/nrmicro2490.

4) Atif SM, Winter SE, Winter MG, McSorley SJ, Baumler AJ. Salmonella enterica serovar typhi
impairs CD4 T cell responses by reducing antigen availability. Infect Immun. 2014;82(6):2247-2254.

5) Costerton JW, Lewandowski Z, Caldwell DE, Korber DR, Lappin-Scott HM. Microbial
biofilms. Annu Rev Microbiol. 1995;49:711-745.

6) Crawford, R. W. et al. Gallstones play a significant role in Salmonella spp. gallbladder colonization and carriage. Proc. Natl. Acad. Sci. U. S. A. 107, 4353-4358 (2010).

7) Dutta U, Garg PK, Kumar R, Tandon RK. Typhoid carriers among patients with gallstones are at increased risk for carcinoma of the gallbladder. Am J Gastroenterol. 2000;95(3):784-787.

8) Datsenko KA, Wanner BL. One-step inactivation of chromosomal genes in escherichia coli K-12 using PCR products. *Proc Natl Acad Sci U S A*. 2000;97(12):6640-6645.

9) Cherepanov PP, Wackernagel W. Gene disruption in escherichia coli: TcR and KmR cassettes with the option of flp-catalyzed excision of the antibiotic-resistance determinant. *Gene*. 1995;158(1):9-14.

10) Holt KE, Parkhill J, Mazzoni CJ, et al. High-throughput sequencing provides insights into genome variation and evolution in salmonella typhi. *Nat Genet*. 2008;40(8):987-993

11) Baddam R, Kumar N, Shaik S, Lankapalli AK, Ahmed N. Genome dynamics and evolution of salmonella typhi strains from the typhoid-endemic zones. *Sci Rep*. 2014;4:7457.

12) Yap KP, Gan HM, Teh CS, Chai LC, Thong KL. Comparative genomics of closely related salmonella enterica serovar typhi strains reveals genome dynamics and the acquisition of novel pathogenic elements. *BMC Genomics*. 2014;15:1007-2164-15-1007

13) Matthews TD, Rabsch W, Maloy S. Chromosomal rearrangements in salmonella enterica serovar typhi strains isolated from asymptomatic human carriers. *MBio*. 2011;2(3):e00060-11

14) Matthews TD, Rabsch W, Maloy S. Chromosomal rearrangements in salmonella enterica serovar typhi strains isolated from asymptomatic human carriers. *MBio*. 2011;2(3):e00060-11

15) Robbins JD, Robbins JB. Reexamination of the protective role of the capsular polysaccharide (vi
antigen) of salmonella typhi. J Infect Dis. 1984;150(3):436-449

16) Raffatellu M, Chessa D, Wilson RP, Dusold R, Rubino S, Baumler AJ. The vi capsular antigen of salmonella enterica serotype typhi reduces toll-like receptor-dependent interleukin-8 expression in the intestinal mucosa. *Infect Immun*. 2005;73(6):3367-3374

17) Wangdi T, Lee CY, Spees AM, et al. The vi capsular polysaccharide enables salmonella enterica serovar typhi to evade microbe-guided neutrophil chemotaxis. *PLoS Pathog*. 2014;10(8):e1004306

18) Wilson RP, Winter SE, Spees AM, et al. The vi capsular polysaccharide prevents complement receptor 3-mediated clearance of salmonella enterica serotype typhi. *Infect Immun*. 2011;79(2):830-837

19) Maldonado RF, Sá-Correia I, Valvano MA. Lipopolysaccharide modification in Gram-negative bacteria during chronic infection. Whitfield C, ed. *FEMS Microbiology Reviews*. 2016;40(4):480-493. doi:10.1093/femsre/fuw007.

20) Baker S, Sarwar Y, Aziz H, et al. Detection of vi-negative salmonella enterica serovar typhi in the peripheral blood of patients with typhoid fever in the faisalabad region of pakistan. *J Clin Microbiol*. 2005;43(9):4418-4425

21) Van der Woude MW, Bäumler AJ. Phase and Antigenic Variation in Bacteria. *Clinical Microbiology Reviews*. 2004;17(3):581-611. doi:10.1128/CMR.17.3.581-611.2004.

22) Ciofu O, Mandsberg LF, Bjarnsholt T, Wassermann T, Hoiby N. Genetic adaptation of pseudomonas aeruginosa during chronic lung infection of patients with cystic fibrosis: Strong and weak mutators with heterogeneous genetic backgrounds emerge in mucA and/or lasR mutants. *Microbiology*. 2010;156(Pt 4):1108-1119.

23) Austin JW, Sanders G, Kay WW, Collinson SK. Thin aggregative fimbriae enhance salmonella enteritidis biofilm formation. *FEMS Microbiol Lett*. 1998;162(2):295-301.

24) Barnhart MM, Chapman MR. Curli biogenesis and function. *Annu Rev Microbiol*. 2006;60:131-147.

25) Humphries AD, Townsend SM, Kingsley RA, Nicholson TL, Tsolis RM, Baumler AJ. Role of fimbriae as antigens and intestinal colonization factors of salmonella serovars. *FEMS Microbiol Lett*. 2001;201(2):121-125.

26) Zogaj X, Bokranz W, Nimtz M, Romling U. Production of cellulose and curli fimbriae by members of the family enterobacteriaceae isolated from the human gastrointestinal tract. *Infect Immun*. 2003;71(7):4151-4158.

27) Zogaj X, Bokranz W, Nimtz M, Romling U. Production of cellulose and curli fimbriae by members of the family enterobacteriaceae isolated from the human gastrointestinal tract. *Infect Immun*. 2003;71(7):4151-4158.